ELSEVIER

Food Chemistry 68 (2000) 21–28

Food Chemistry

www.elsevier.com/locate/foodchem

A critical appraisal of the kinetic model for the Maillard browning of glucose with glycine

L.P. Leong, B.L. Wedzicha*

Procter Department of Food Science, University of Leeds, Leeds LS2 9JT, UK

Received 11 January 1999; received in revised form 20 May 1999; accepted 20 May 1999

Abstract

A critical analysis of kinetic data for the loss of sulphite species, S(IV), in the glucose-glycine–S(IV) reaction, and the browning (A_{470}) of glucose–glycine mixtures (pH 5.5, 0.2 mol l^{-1} acetate buffer, 55°C) confirm the accuracy of the 3-step model (proposed by Davies, C.G.A., Wedzicha, B.L., & Gillard, C. 1997). (Kinetic model of glucose–glycine reaction. *Food Chemisty*, *60*, 323–329). Rate constants k_1 and k_2 are obtained by regression of [S(IV)]-time data to the integrated rate equation for the glucose–glycine–S(IV) reaction. It is confirmed that neither rate constant depends on [S(IV)]. The integrated rate equation for the overall browning reaction is derived, and the rate constant k_3 for melanoidin formation as well as the effective extinction coefficient E are obtained by regression. The value of E is confirmed for high molecular weight ($M_r > 3500$) melanoidins by a radiochemical technique based on ^{14}C-labelled glucose. This paper thus presents a protocol to obtain values of the significant rate constants in the browning of aldoses with amino acids. © 1999 Elsevier Science Ltd. All rights reserved.

1. Introduction

The initial reaction of an aldose with an amino compound is followed by a cascade of consecutive and parallel reactions to form a large range of low and high molecular weight products. It has been known for some time (Haugaard, Tumerman & Silvestri, 1951; Kato, Yamamoto & Fujimaki, 1969) that the overall kinetics of colour formation (measured in terms of absorbance at a single wavelength) are relatively straightforward, and can be described by a three rate determining step consecutive mechanism. Davies, Wedzicha and Gillard (1977) showed how to measure the individual rate constants in such a mechanism without having to interpolate all three steps from absorbance-time data. They used the reaction of sulphite species S(IV) with a key reactive intermediate in the browning reaction to trap this intermediate and hence deduce the rate of its formation.

The present investigation begins with a review of progress in the application of this approach to the study of the kinetics of Maillard browning, and this is followed by a further refinement of the kinetic model as our thinking has become more mature.

2. Critical appraisal of the evolving kinetic model

The group at Leeds follows the kinetics of browning mostly at pH 5.5 and 55°C. This pH value is in the middle of the pH range of many plant and animal foods. This temperature is often used in accelerated storage trials. Other investigations at Leeds (Davies et al., 1997; Wedzicha & Kedward, 1995) have shown that the kinetics of browning remain unchanged if the temperature is increased to 70 and 100°C, and the models are, therefore, expected to apply to the moderate thermal treatment of foods, e.g. dehydration, and to long term food storage. At pH 5.5, the major pathway in browning is the 3-deoxyosulose route (Tressl, Nittka, Kersten, & Rewicki, 1995); in the browning reaction of glucose, the key intermediate is 3-deoxyhexosulose, DH, which is formed from the 1,2-enaminol precursor of the Amadori compound. The intermediate which is most reactive towards browning along this route is the α,β-unsaturated carbonyl compound 3,4-dideoxyhexosulos-3-ene, DDH. The mechanism by which S(IV) inhibits the browning reaction at pH 5.5 has been established rigorously (McWeeny, Knowles & Hearne, 1974; Wedzicha & Garner, 1991; Wedzicha & Kaban, 1986) as the reaction of DDH with sulphite ion to form 3,4-dideoxy-4-sulphohexosulose, DSH. This reaction, therefore, leads to

* Corresponding author. Tel.: +44-(0)113-233-2959; fax: +44-(0)113-233-2982.

0308-8146/99/$ - see front matter © 1999 Elsevier Science Ltd. All rights reserved.
PII: S0308-8146(99)00146-6

the irreversible binding of S(IV). The kinetics of the glucose–glycine–S(IV) reaction reveal two rate-determining steps. The first is the formation of DH whereas the second is the conversion of DH to some activated complex which may resemble DDH (Davies et al., 1997).

The approach used by Davies et al. (1997) is based on the assumption that, in the presence of S(IV), the glucose–glycine browning reaction is diverted towards the relatively unreactive DSH, whilst, in the absence of S(IV), the reaction continues towards melanoidins; the rates of the first two steps are the same whether S(IV) is present or not. This thinking is summarised in Fig. 1. Thus, the rate of reaction of S(IV) in a glucose–glycine–S(IV) reaction provides the route to obtaining the values of the rate constants k_1 and k_2. A particular feature of the analysis of [S(IV)]-time data is that there appears to exist a dependence of the rate constant k_1 on the initial S(IV) concentration (Davies et al., 1997; Wedzicha & Kedward, 1995; Wedzicha & Vakalis, 1988). This is apparent when values of k_1 are obtained as the slope of the linear portion of such concentration-time curves. The mathematical justification for this approach is that the reaction should reach a steady-state situation, with the rate of formation of DH being equal to the rate of its loss, to give a constant rate of reaction of S(IV). In general, values of k_1, measured in this way, increase linearly with initial S(IV) concentration. There is a plausible explanation of this dependence in terms of the acid-base behaviour of HSO_3^-/SO_3^{2-} on the steps leading up to the formation of DH (Wedzicha & Vakalis).

The integrated rate equation for the change, with time, of [S(IV)] in the glucose–glycine–S(IV) reaction, with [glucose]≈[glycine]≫[S(IV)], is

$$[S(IV)]_t = [S(IV)]_0 - k_1 t + \frac{k_1}{k_2}(1 - e^{-k_2 t}) \quad (1)$$

when derived (Wedzicha, 1984) without including any kinetic effect of S(IV) on k_1. Nevertheless, the equation is found to fit individual kinetic runs very well (Wedzicha). It is possible, however, that its use for the fitting of data is not sufficiently sensitive to flag up the dependence of k_1 on [S(IV)] as a systematic deviation of the experimental data from calculated [S(IV)]-time curves. This issue is central to the calculation of values of all three rate constants for the kinetic model investigated by Davies et al. (1997) and has to be resolved unequivocally.

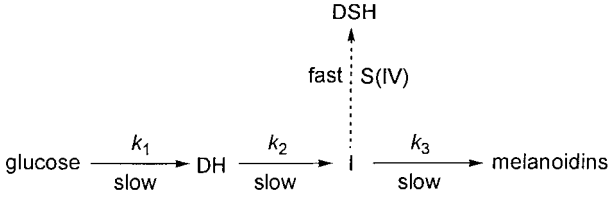

Fig. 1. A kinetic model for the glucose-glycine browning reaction (Davies et al., 1997) showing the point at which the reaction is inhibited by sulphite species, S(IV). DH is 3-deoxyhexosulose, DSH is 3,4-dideoxy-4-sulphohexosulose, and I is an unspecified intermediate.

The kinetic model developed by Davies et al. (1997) is based on the production of melanoidins whose molar extinction coefficient remains constant throughout the observation period (up to an absorbance of 2 units). Whereas the molecular weights of melanoidins are expected to span a very wide range of values, their molar extinction coefficient can be expressed simply in terms of the concentration of glucose molecules converted into melanoidins. On this basis, measurement of the extent of browning (A_{470}) of DH (the key intermediate in the conversion of glucose to melanoidins) suggests that this value is 1030 mol^{-1} l cm^{-1} (Davies et al.), but it has not been possible to measure this value directly for melanoidins from glucose. It is envisaged that, from the point of view of colour, melanoidins could be built up of sub-units in two contrasting ways. (i) Low molecular weight moieties (which may inherently be coloured or not) combine and, as a consequence of their reaction, the chromophore is altered considerably, e.g. through extended conjugation within the polymer. (ii) The coloured low molecular weight moieties combine in such a way that the chromophores are isolated from one another. The latter type of polymerisation reaction is more likely to give rise to melanoidins whose "molar" extinction coefficient is independent of polymer length and constant as the browning reaction proceeds. All that is changing is the concentration of these sub-units either individually or combined. Wedzicha and Kaputo (1987, 1992) in fact proposed such a structure on the basis of the extent of bleaching of melanoidins by S(IV) in relation to their sulphur-to-carbon ratios. Although discrete coloured low molecular weight products are known to be present in melanoidin mixtures (Ames, Bailey & Mann, 1999), the products in the glucose–glycine reaction (pH 5) appear to be dominated by brown polymers (Bailey, Ames & Monti, 1996), possibly pointing to a relatively homogeneous mixture of products with regard to their absorbance characteristics.

Davies et al. (1997) investigated the kinetic dependence on concentration of the individual steps in the glucose–glycine reaction, and identified the following series of rate equations.

$$\frac{d[DH]}{dt} = k_1 \quad (2)$$

$$\frac{d[I]}{dt} = k_2[DH] \quad (3)$$

$$\frac{dA_{450}}{dt} = k_3[I] \quad (4)$$

where k_1, k_2 and k_3 are rate constants with the same meaning as in Fig. 1. These pseudo order rate constants apply when [glucose] and [glycine] are so large that they can be considered as constant during the observation period. In addition, the absorbance of reaction mixtures is related to the molar extinction coefficient of the melanoidins, E, and their concentration [M] in terms of glucose molecules converted, by,

$$A_{450} = E[\mathrm{M}] \tag{5}$$

when measured in a 1 cm cell. A particular reason for the investigation carried out by Davies et al. was to explain our observation that the absorbance of glucose-amino acid reaction mixtures appeared to vary with $(\text{time})^3$. This could be reconciled easily if one made the assumption that the extent of conversion of the reaction intermediate, I, to melanoidin was small, i.e. that the concentration of this intermediate remained equal to that which was formed in the preceding reactions. Thus, the absorbance-time data could be modelled simply as,

$$(A_{450})_t \approx k_3 \int k_1 t - \frac{k_1}{k_2}(1 - \mathrm{e}^{-k_2 t})\mathrm{d}t \tag{6}$$

and, by neglecting terms beyond t^3 in the expansion of $\mathrm{e}^{-k_2 t}$, one obtains the result that,

$$(A_{450})_t \approx \frac{k_1 k_2 k_3}{6} t^3 \tag{7}$$

Whilst this approximation provides a good basis for discussing the kinetics of the glucose-glycine reaction, we now feel that it is unsatisfactory for the most accurate work for two reasons. (i) Absorbance-$(\text{time})^3$ plots obtained for reactions carried out at 55°C consistently show slight curvature (Wedzicha & Leong, 1998a, 1998b). (ii) The second reason can be appreciated by examining Table 1. This shows values of the concentrations of DH, I and melanoidin, and the final absorbance, calculated by numerical integration of the set of 3 rate equations given above with $k_1 = 7.0 \times 10^{-4}$ mol l^{-1} h^{-1}, $k_2 = 0.17$ h^{-1}, $k_3 = 0.0874$ h^{-1} and $E = 1030$ mol l^{-1} l cm^{-1}, i.e. the values obtained by Davies et al. (1997) for [glucose] = 1 mol l^{-1} and [glycine] = 0.5 mol l^{-1}. Thus, we see that the amount of I converted to melanoidins is significant (the concentrations of the two species are of the same magnitude) and the assumption that [M] can be neglected in relation to [I] is not strictly true, except at short reaction times. Besides this, the data confirm that the conversion of glucose to intermediates DH and I, and melanoidins, is small compared with the concentration of glucose and glycine, and the pseudo-order rate constants are expected to apply.

Table 1
Numerical integration of rate equations for the glocose–glycine reaction with $k_1 = 7 \times 10^{-4}$ mol l^{-1} l^{-1} h^{-1}, $k_2 = 9.17$ h^{-1}, $k_3 = 0.0874$ h^{-1} and $E = 1030$ mol l^{-1} l cm^{-1} (at 450 nm) for [glucose] = 1 mol l^{-1} and [glycine] = 0.5 mol l^{-1}, pH 5.5, 55°C[a]

Time/h	[DH]/mmol l^{-1}	[I] mmol l^{-1}	[M]/mmol l^{-1}	Absorbance
2	1.19	0.201	0.012	0.013
4	2.03	0.682	0.087	0.089
6	2.63	1.31	0.259	0.267
8	3.06	1.99	0.547	0.564
10	3.36	2.68	0.956	0.984
12	3.58	3.34	1.48	1.53
14	3.74	3.94	2.12	2.18

[a] The absorbance is calculated for 450 nm, which was the wavelength use by Davies et al. (1997).

The introductory themes highlight the fact that, whilst we have an excellent kinetic model, which reconciles well the time and concentration dependence of the glucose–glycine reaction at small absorbances, it leaves a number of questions unanswered. Specifically,

- does S(IV) exert a kinetic effect on the process described by k_1,
- is a single value of molar extinction coefficient applicable to the coloured products of the browning reaction,
- does the full analytical solution to the rate equations provide a more detailed description of the reaction than the approximate solution used so far?

The aim of this paper is to address these concerns and provide the most rigorous analysis of new data to consolidate the proposed model.

3. Materials and methods

All chemicals were of analytical grade and were obtained from Sigma or Aldrich. Radiolabelled substances were obtained from Amersham International.

3.1. General procedure used for kinetic studies

Stock buffer was prepared to give a final concentration of 2 mol l^{-1} of sodium acetate with sufficient glacial acetic acid to give pH 5.5. Reaction mixtures were prepared by dissolving solids in water (75% of final volume) to give a final concentration of 1 mol l^{-1} glucose and 0.5 mol l^{-1} glycine. Stock acetate buffer (10% of final volume) was added and the pH of the mixture readjusted to 5.5 with NaOH/acetic acid. For experiments involving S(IV), a given weight of sodium metabisulphite was dissolved in the reaction mixture to give a final S(IV) concentration of 0.02–0.1 mol l^{-1}. Reaction mixtures were made up to the final volume with water. The reaction was started by placing the solutions in a

water bath maintained at 55°C and aliquots were withdrawn at timed intervals for analysis. Absorbance measurements were made at 470 nm. The concentration of total S(IV) was measured by the procedure of Humphrey, Ward, and Hinze (1970), using 5,5′-dithiobis(2-nitrobenzoic acid) (Ellman's reagent, DTNB) dissolved in phosphate buffer, as described previously by this Group (e.g. Davies et al., 1997; Wedzicha & Kedward, 1995). Solutions of S(IV) were standardised by iodimetric titration.

3.2. Rate of reaction of glucose

Aliquots (200 μl) of the glucose–glycine–S(IV) reaction mixture were withdrawn at timed intervals and added to phosphate buffer (1 ml, pH 8, 0.1 mol l^{-1}) before making up to 100 ml with water. The glucose concentration was measured by taking an aliquot (100 μl) of this solution and mixing with the reagents in the glucose enzyme assay kit supplied by Boehringer Mannheim.

3.3. Radiochemical investigations

A reaction mixture (25 ml) was prepared without S(IV) as described above. However, before making up to the final volume, a negligible mass of (uniformly labelled) U-^{14}C-glucose was added to the solution. The activity of ^{14}C in the reaction mixture was 1.85 MBq. A parallel experiment without the radiolabelled chemical was run to measure the rate of browning at 470 nm. Aliquots (2 ml) of each reaction mixture were withdrawn and dialysed against running water in 3 ml capacity dialysis cassettes (Pierce & Warriner, UK) with a stated molecular weight cut off of 3500 daltons. After a minimum dialysis time of 10 days, the retentates in the cassettes were removed, washed out with water and made up to 10 ml with water. The absorbance of each solution was measured at 470 nm. Aliquots (1 ml), from the labelled reaction, were mixed with scintillation fluid (10 ml) (Emulsifier Scintillator Plus, Packard, UK) in separate glass vials, and counted using a Packard Tri-Carb 1900TR scintillation counter. Quenching was corrected using an internal standard.

4. Results and discussion

4.1. The glucose–glycine–S(IV) reaction

We begin this investigation by considering the family of [S(IV)]-time plots for glucose–glycine–S(IV) reactions at different initial S(IV) concentrations, obtained in the present work and shown in Fig. 2. Multiple regression (Microcal Origin 4, Aston Scientific Ltd., Buckinghamshire, England) of these data to equation 1 by "sharing" the values of k_1 and k_2, but otherwise allowing them and the values of $[S(IV)]_0$ to vary to produce the best fit, allows us to test the possibility that the reaction is independent of [S(IV)] concentration. The lines drawn through the data points in Fig. 2 are the best fits, which are obtained when $k_1 = (5.34 \pm 0.48) \times 10^{-4}$ mol l^{-1} h^{-1} and $k_2 = (1.92 \pm 0.22) \times 10^{-3}$ h^{-1}. Since there are no systematic deviations between experimental and calculated values, it is inferred that loss of S(IV) in this reaction is indeed independent of [S(IV)], i.e. Eq. (1) fits well the whole set of data.

It is informative to explore the reason why the previous mathematical approach gave rise apparently to a first order dependence of k_1 on [S(IV)]. From Eq. (1), the time t_{S0} required for the concentration of S(IV) to reduce to zero is given by,

$$[S(IV)]_0 k_1 t_{S0} - \frac{k_1}{k_2}(1 - e^{-k_2 t_{S0}}) \quad (8)$$

and the rate of loss of S(IV) at this moment is given by,

$$-\frac{d[S(IV)]}{dt} = k_1(1 - e^{-k_2 t_{S0}}) \quad (9)$$

Using the values of k_1 and k_2 determined above, the values of t_{S0} are calculated using Eq. 8 to be 211, 307, 384, 452 and 514 h for $[S(IV)]_0 = 0.02$, 0.04, 0.06, 0.08 and 0.10 mol l^{-1}, respectively. Thus, the rate of loss of S(IV), as $[S(IV)] \rightarrow 0$, varies with $[S(IV)]_0$ as shown in Fig. 3, where a straight line has been drawn through the data points according to previous practice, despite it now being evident that the actual graph is curved. Typically, such graphs would in the past have consisted of 5 data points over this concentration range; close inspection of our previous data indicates that such plots have frequently shown slight curvature. When the

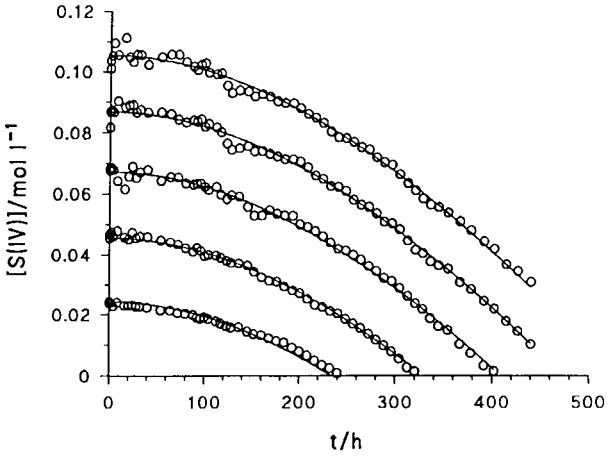

Fig. 2. [S(IV)]-time data for the glucose-glycine-S(IV) reaction at different initial S(IV) concentrations. Reaction conditions: [glucose] = 1 mol l^{-1}; [glycine] = 0.5 mol l^{-1}; pH 5.5 (0.2 mol l^{-1} acetate buffer); 55°C. The lines drawn through the data points are calculated after multiple regression to the integrated rate equation.

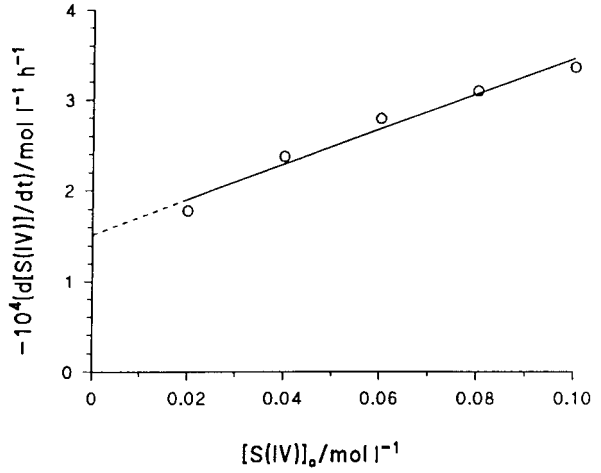

Fig. 3. Simulated plot of the value of k_1 (the slope of [S(IV)]-time plots as [S(IV)]→0) vs initial S(IV) concentration $[S(IV)]_0$, to reproduce the previously used method of calculating this rate constant.

straight line is extrapolated to $[S(IV)]_0 = 0$, in order to obtain k_1, the intercept (1.52×10^{-4} mol l^{-1} h^{-1}) is much lower than the true value of k_1, i.e. 5.34×10^{-4} mol l^{-1} h^{-1}). We recently (Wedzicha & Leong, 1998a, 1998b) reported the value of k_1 as 1.62×10^{-4} mol l^{-1} h^{-1} using this method of calculation. Thus, it is possible to work backwards from the correct values of rate constants to estimate those which had previously been calculated by extrapolation.

The slope of the rate-$[S(IV)]_0$ graph was previously taken to be the rate constant for the S(IV)-dependent process; here the value of the slope (1.93×10^{-3} h^{-1}) is in fact close to the true value of k_2 (1.92×10^{-3} h^{-1}). Since plots of rate of loss of S(IV) vs $[S(IV)]_0$ obtained in this way are not linear, we suggest that they offer no useful route to the calculation of rate constants k_1 and k_2. The reason for the failure of the earlier approach is because the steady-state condition requiring for it to be valid is not established within the observation period. Instead, we advocate the use of multiple non-linear regression to Eq. 1. If only a single data-set is used for regression, it is best for the results to have been obtained at a relatively high $[S(IV)]_0$ because the longer reaction times required to gather the necessary data provide more information about the contributions of k_1 and k_2 to the overall kinetics.

The glucose concentration was measured enzymatically during the course of the glucose–glycine–S(IV) reaction. Control experiments showed that there was no interference with the analysis from S(IV) after dilution. We note with interest that, during the observation period as [S(IV)] falls to zero, the rate of loss of glucose is constant at 5.32×10^{-4} mol l^{-1} h^{-1}, i.e. at the same rate as the value of k_1. This adds credence to the approach and numerical analysis adopted here, and points to the fact that, in our system, the reactivity of glucose is accounted for completely by its conversion in the first rate-limiting step of the kinetic model.

4.2. Kinetics of browning

The rate equations for the individual steps in the model of the browning reaction allow the following equations for the loss of glucose, G, the formation of melanoidins, M, and the overall rates of formation of DH and I to be written as follows:

$$-\frac{d[G]}{dt} = k_1 \tag{10}$$

$$\frac{d[DH]}{dt} = k_1 - k_2[DH] \tag{11}$$

$$\frac{d[I]}{dt} = k_2[DH] - k_3[I] \tag{12}$$

$$\frac{d[M]}{dt} = k_3[1] \tag{13}$$

Integration of Eqs. (10–13) in sequence gives the concentration of M as a function of time as,

$$[M] = k_1 t - \frac{k_1}{k_2} - \frac{k_1}{k_3} + \frac{k_1 k_3}{k_2(k_3 - k_2)} e^{-k_2 t} - \frac{k_1 k_2}{k_3(k_3 - k_2)} e^{-k_3 t} \tag{14}$$

This integration is exact and the only assumption which has been made is that the concentrations of glucose and glycine remain constant throughout the observation period. Fig. 4 shows regression of absorbance-time data to the following equation,

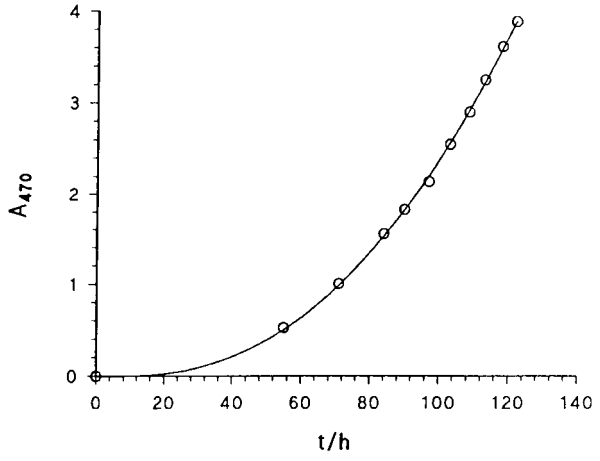

Fig. 4. Regression of absorbance-time data to the integrated rate equation for browning. Reaction conditions: [glucose] = 1.0 mol l^{-1}; [glycine] = 0.5 mol l^{-1}; pH 5.5 (0.2 mol l^{-1} acetate buffer); 55°C. The lines drawn through the data points are calculated from the regression equation.

$$(A_{470})_t = [\mathrm{M}]_t E \quad (15)$$

where $[\mathrm{M}]_t$ is given by Eq. 14. The best fit is obtained when $k_3 = 0.0259 \pm 0.0015$ h^{-1} and $E = 972 \pm 29$ mol^{-1} l cm^{-1}. The fit of experiment to theory is seen to be excellent and we conclude that the values of k_1, k_2, k_3 and E reported here are the best available, because their derivation is based on a rigorous treatment of the kinetic data. It is important to note that the kinetic data can be modelled accurately by assuming that there is a single value of E which applies over the whole observation period.

The simultaneous use of Eqs. (14) and (15) allowed the value of E to be computed, in contrast to the previous application of the approximate solution given as Eq. 7, where only the composite parameter, k_3E, could be derived. Nevertheless, the first approximation (neglecting terms above $k_2^3t^3$ in the expansion of e^{-k_2t}) to Eq. 14 gives the same result as that deduced by Davies et al. (1997) from a different viewpoint, i.e.

$$[\mathrm{M}] = \frac{k_1k_2k_3}{6}t^3 \quad (16)$$

which is to be expected if the outcome is to be consistent with the general observation that absorbance vs t^3 graphs are approximately linear at small values of absorbance. In the present work, the absorbance data (at 470 nm) are seen to be modelled well up to an absorbance of 4, which is well out of the range of the approximate solution. The higher the absorbance to which the reaction is followed, the more accurate will be the value of E which is calculated.

4.3. Extinction coefficients of melanoidins

The experiments used to obtain the absorbance-time data given in Fig. 4 were repeated with the glucose labelled uniformly with ^{14}C, and melanoidins were separated by dialysis (nominal molecular weight cut-off with reference to protein $M_r > 3500$). We will distinguish the fractions which have $M_r < 3500$ from those which have $M_r > 3500$ by referring to the low and high molecular weight fractions, respectively. Assuming that 1 mol of melanoidin corresponds to the conversion of 6 carbon atoms from glucose into the polymer, the ^{14}C-activity of the melanoidin, together with the specific activity of the glucose, may be used to calculate the molar concentration in the high molecular weight fraction. At pH 5.5, significant retro-aldolisation of the sugar, DH and other intermediates can occur with the formation of short chain reactive carbonyl compounds. The definition of the concentration of melanoidins adopted here takes account of the possible incorporation of such sugar fragments into melanoidins. The relationship of the absorbance of this melanoidin fraction to the concentration of "melanoidin" is shown in Fig. 5 where a change in melanoidin concentration is the result of a corresponding change in the extent of reaction. It is not simply a step-wise dilution of a pre-formed melanoidin as one would use to test for adherence to the Beer-Lambert law.

The result indicates that, over the observation period, i.e. as the overall absorbance of reaction mixtures at 470 nm increases to 4, the extinction coefficient of the high molecular weight melanoidins remains approximately constant. Whilst this graph appears slightly curved, we will consider here a linear approximation. The best line through the data passes close to the origin and the value of $E = 940$ mol^{-1} l cm^{-1} is deduced from the slope. This value is in remarkable agreement with the value obtained above (972 mol^{-1} l cm^{-1}) for whole reaction mixtures using kinetic considerations alone. Davies et al. (1997) estimated the value of E at 450 nm for the DH-glycine reaction to be 1030 mol^{-1} l cm^{-1}. The melanoidins formed in this way have $A_{470}/A_{450} \approx 0.92$, which means that the value of E at 470 nm should be 950 mol^{-1} l cm^{-1}. It is encouraging to see that three methods of determining E based on quite different reasoning and theory give such consistent results. Since the high molecular weight melanoidin fraction contributes only up to 10% of the absorbance of the reaction mixtures, we can conclude that the apparent extinction coefficient of the low molecular weight fraction must be the same and that it remains effectively constant throughout the observation period. The proportion of melanoidins to total coloured material is expected to change with temperature, time, reactant concentration and pH. The value of 10% referred to above is, therefore, only relevant for the system and conditions under discussion. At present we have no access to specific melanoidin fractions to test this conclusion more rigorously. Plots similar to that shown in Fig. 5, but for melanoidins

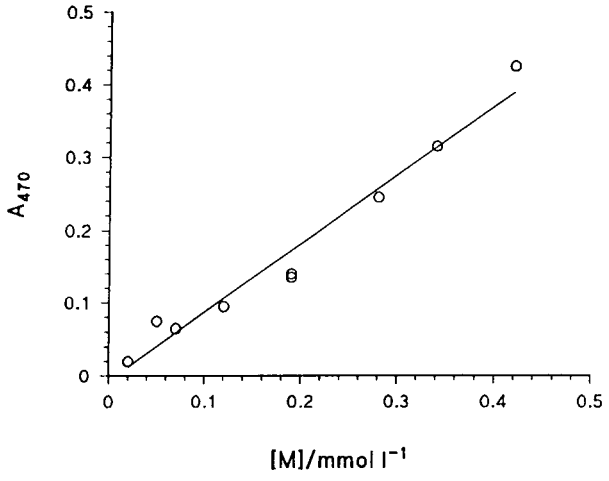

Fig. 5. Relationship of absorbance at 470 nm to the concentration of glucose converted to melanoidins [M] with $M_r > 3500$.

obtained from glutamic acid, serine and valine, are excellent straight lines which pass through the origin and will be reported elsewhere (Leong & Wedzicha, unpublished).

We note with interest the work of Hofmann (1998) who prepared melanoidins from glucose and glycine (pH 7, 95°C, 4 h) and subsequently fractionated these by filtration. The colour impact of each fraction was reported as the colour dilution factor, obtained by diluting the melanoidin solution with water until the colour was just detectable visually in a triangle test using water as a blank. This author reports only traces (6 mg out of a total of 793 mg) of melanoidins with $M_r > 3000$, but a significant amount (155 mg) with $1000 < M_r < 3000$. If one divides the colour dilution factor (as a measure of absorbance) by the mass of melanoidin in solution, values of 1500, 830 and 1600 g^{-1} were obtained for melanoidins with M_r of 3000–10000, 1000-3000 and < 1000, respectively. The dilution factor was obtained by binary dilution of melanoidin solutions and, if we assume that the uncertainty in this factor is one dilution step, i.e. a factor of 2, then the values calculated above are all deemed to be similar. Hence, we suggest that the results reported by Hofmann are consistent with our finding that melanoidins of different molecular weights have similar extinction coefficients.

4.4. Conversion of low molecular weight coloured products into high molecular weight products

Fig. 6 shows the way that the absorbance at 470 nm changes with time for the low and high molecular weight melanoidin fractions. Here, absorbance has been plotted as a function of t^3 because, in this form, it provides appropriate weighting of the concentration data

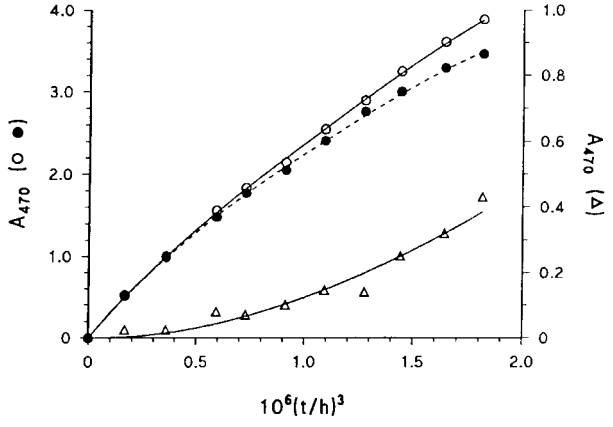

Fig. 6. Simulation of the conversion of low molecular weight ($M_r < 3500$) melanoidins into high molecular weight ($M_r > 3500$) melanoidins. ○ total melanoidin; ● low molecular weight melanoidin; △ high molecular weight melanoidin. The lines drawn through the experimental data points are calculated by regression to the integrated rate equations.

with respect to time for the comparison of trends by inspection. A possible route to the high molecular weight product is the further polymerisation of the low molecular weight product. The simplest mechanism for this process could be a combination of two low molecular weight components in a bimolecular reaction step. Thus, we speculate that the kinetics of melanoidin formation are given more explicitly by,

$$\frac{d[M1]}{dt} = k_3[I] - k_4[M1]^2 \quad (17)$$

$$\frac{d[M2]}{dt} = k_4[M1]^2 \quad (18)$$

where M1 and M2 are melanoidin components below and above the molecular weight limit of the dialysis membrane, respectively, and k_3 and k_4 are the corresponding rate constants for their formation. Eq. 18 describes the process which moves a component from being below this molecular weight to above. Since M1 and M2 cannot be distinguished by their absorbance characteristics and are deemed to have the same extinction coefficient, the absorbance of the whole reaction mixture is, therefore $E[M] = E([M1] + 2[M2])$. Thus, the value of k_3 should be the same as calculated from the kinetic model for the formation of M, i.e. 0.0259 h^{-1}. Simultaneous numerical integration of Eqs. (10), (11),(12),(17) and (18), using the established rate constants and extinction coefficient, and with k_4 as the only adjustable parameter (equal to 1.39 mol^{-1} l h^{-1} for the best fit) gives predicted absorbance time data as plotted in the form of the lines passing through the experimental points in Fig. 6. Thus, we see that this type of kinetic approach can account well for the distribution of the low and high molecular weight fractions. There are, of course, many other mechanisms which convert M1 to a component of the high molecular weight fraction. An example is the single step whereby M1 reacts with a molecule of I. The example considered in detail above is meant to be indicative of the need for a further rate-limiting step rather than to present an unequivocal solution. Already the calculation stretches the precision of the data. Currently we are using MALDI-TOF mass spectrometry to investigate the possible stepwise generation of melanoidins in relation to the kinetic data presented above.

5. Conclusion

The rigorous analysis of kinetic data for the browning of glucose + glycine, based on the model proposed by Davies et al. (1997) leads to the following conclusions which modify the approach used to derive individual rate constants.

(i) The 3-step model for the browning of glucose + glycine is accurate.

(ii) The rate of the glucose–glycine–S(IV) reaction is independent of [S(IV)], and rate constants can be obtained simply by non-linear regression of experimental [S(IV)]-time data to the integrated rate expression,

$$[\mathrm{S(IV)}]_t = [\mathrm{S(IV)}]_0 - k_1 t + \frac{k_1}{k_2}(1 - \mathrm{e}^{-k_2 t})$$

(iii) Absorbance-time data can be fitted using the rate constants k_1 and k_2 derived in (ii) above together with *unique* values of k_3 and extinction coefficient E, by means of the following integrated rate equation,

$$(A_{470})_t = E\left\{k_1 t - \frac{k_1}{k_2} - \frac{k_1}{k_3} + \frac{k_1 k_3}{k_2(k_3 - k_2)}\mathrm{e}^{-k_2 t} - \frac{k_1 k_2}{k_3(k_3 - k_2)}\mathrm{e}^{-k_3 t}\right\}$$

Acknowledgements

The authors are very grateful to Tiny van Boekel for his many helpful comments. The results which are reported in this paper are from research which has been carried out with financial support from the Commission of the European Communities, Agriculture and Fisheries (FAIR) specific RTD programme, CT96-1080, "Optimization of the Maillard Reaction. A Way to Improve the Quality and Safety of Thermally Processed Foods". It does not necessarily reflect its views and in no way anticipates the Commission's future policy in this area.

References

Ames, J. M., Bailey, R. G., & Mann, J. (1999). Analysis of furanone, pyranone and new heterocyclic coloured compounds from sugar-glycine Model Maillard Systems. *Journal of Agricultural and Food Chemistry*, *47*, 438–443.

Bailey, R. G., Ames, J. M., & Monti, S. M. (1996). An analysis of the non-volatile reaction products of aqueous Maillard model systems at pH 5, using reversed-phase HPLC with diode-array detection. *Journal of the Science of Food and Agriculture, 72*, 97–103.

Davies, C. G. A., Wedzicha, B. L., & Gillard, C. (1997). Kinetic model of the glucose–glycine reaction. *Food Chemistry, 60*, 323–329.

Haugaard, G., Tumerman, L., & Silvestri, H. (1951). A study of the reaction of aldoses with amino acids. *Journal of the American Chemical Society, 73*, 4594–4600.

Hofmann, T. (1998). Studies on the relationship between molecular weight and the color potency of fractions obtained by thermal treatment of glucose/amino acid and glucose/protein solutions by using ultracentrifugation and color dilution techniques. *Journal of Agricultural and Food Chemistry, 46*, 3891–3895.

Humphrey, R. E., Ward, M. H., & Hinze, W. (1970). Spectrophotometric determination of sulphite with 4,4′-dithiopyridine and 5,5′-dithiobis(2-nitrobenzoic acid). *Analytical Chemistry, 42*, 698–702.

Kato, H., Yamamoto, M., & Fujimaki, M. (1969). Mechanisms of browning degradation of D-fructose in special comparison with D-glucose–glycine reaction. *Agricultural and Biological Chemistry, 33*, 939–948.

McWeeny, D. J., Knowles, M. E., & Hearne, J. F. (1974). The chemistry of non-enzymic browning in foods and its control by sulphites. *Journal of the Science of Food and Agriculture, 25*, 735–746.

Tressl, R., Nittka, C., Kersten, E., & Rewicki, D. (1995). Formation of isoleucine-specific Maillard products from [1-^{13}C]-D-glucose and [1-^{13}C]-D-fructose. *Journal of Agricultural and Food Chemistry, 43*, 1163–1169.

Wedzicha, B. L. (1984). A kinetic model for the sulphite-inhibited Maillard reaction. *Food Chemistry, 14*, 173–184.

Wedzicha, B. L., & Garner, D. N. (1991). Formation and reactivity of osuloses in the sulphite-inhibited Maillard reaction of glucose and glycine. *Food Chemistry, 39*, 73–86.

Wedzicha, B. L., & Kaban, J. (1986). Kinetics of the reaction between 3-deoxyhexosulose and sulphur(IV) oxospecies in the presence of glycine. *Food Chemistry, 22*, 209–223.

Wedzicha, B. L., & Kaputo, M. T. (1987). Reaction of melanoidins with sulphur dioxide: stoichiometry of the reaction. *International Journal of Food Science and Technology, 22*, 643–651.

Wedzicha, B. L., & Kaputo, M. T. (1992). Melanoidins from glucose and glycine: composition, characteristics and reactivity towards sulphite ion. *Food Chemisty, 43*, 359–367.

Wedzicha, B. L., & Kedward, C. (1995). Kinetics of the oligosaccharide-glycine-sulphite reaction: relationship to the browning of oligosaccharide mixtures. *Food Chemistry, 54*, 397–402.

Wedzicha, B. L., & Lai Peng Leong (1998a). Modelling and control of Maillard browning. *The European Food and Drink Review* (Spring), 37–42.

Wedzicha, B. L., & Lai Peng Leong (1998b). Modelling of the Maillard reaction: rate constants for individual steps in the reaction. In J. O'Brien, H. E. Nursten, M. J. C. Crabbe, & J. M Ames, *The Maillard reaction in foods and medicine, proceedings of the 6th international conference on the Maillard reaction* (pp. 141–146). Cambridge: The Royal Society of Chemistry.

Wedzicha, B. L., & Vakalis, N. (1998). Kinetics of the sulphite-inhibited Maillard reaction: the effect of sulphite ion. *Food Chemistry, 27*, 259–271.